Journal of Advanced Research 17 (2019) 109–116

Contents lists available at ScienceDirect

Journal of Advanced Research

journal homepage: www.elsevier.com/locate/jare

Original article

Resolution-elastic neutron scattering by correlation techniques

F. Mezei [a,b], M.T. Caccamo [c], F. Migliardo [d,e,*], S. Magazù [f]

[a] European Spallation Source ERIC, Lund, Sweden
[b] HAS Wigner Research Center, Budapest, Hungary
[c] Istituto per i Processi Chimico-Fisici (IPCF)-Consiglio Nazionale delle Ricerche (CNR), Viale F. Stagno D'Alcontres, 37, 98158 Messina, Italy
[d] Department of Chemical, Biological, Pharmaceutical and Environmental Sciences, University of Messina, Viale F. Stagno D'Alcontres, 31, 98166 Messina, Italy
[e] Laboratoire de Chimie Physique, UMR8000, Universitè Paris Sud, 91405 Orsay cedex, France
[f] Department of Mathematical and Informatics Sciences, Physical Sciences and Earth Sciences, University of Messina, Viale F. Stagno D'Alcontres, 31, 98166 Messina, Italy

HIGHLIGHTS

- Resolution-Elastic Neutron Scattering (RENS) is a recently established approach.
- Correlation spectroscopy can be used in pulsed and continuous neutron sources.
- The correlation technique overcomes the limits of weak signals and high background.
- Correlation spectroscopy is an efficient way to perform RENS studies.
- The statistical chopper is realized following a pseudo-random sequence.

GRAPHICAL ABSTRACT

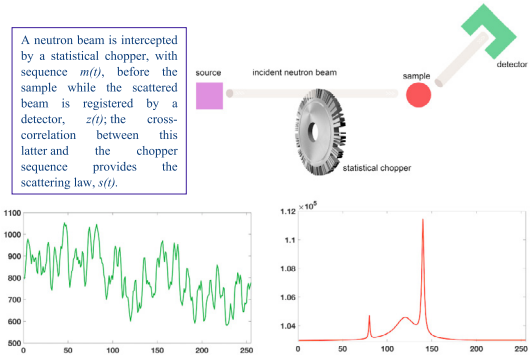

ARTICLE INFO

Article history:
Received 6 November 2018
Revised 15 February 2019
Accepted 15 February 2019
Available online 16 February 2019

Keywords:
Resolution-elastic neutron scattering
Quasi-elastic neutron scattering
Statistical chopper
Correlation spectroscopy
Instrumental resolution
Numerical simulation

ABSTRACT

Neutron scattering applications often require discriminating the elastic contribution from the inelastic contribution. For this purpose, correlation spectroscopy offers an effective tool with both pulsed and continuous neutron sources as well as several advantages: the analysis of the neutron velocity distribution can be carried out with a duty factor of 50%, independently on the resolution value; the best statistical accuracy for spectra where the elastic part encompasses most of the integrated intensity is provided. Depending on the statistical chopper position, correlation analysis can be used for both incoming and outgoing neutron velocity determination. Moreover, the correlation technique is very profitable for investigating weak signals in the presence of high background, which is often the case for small samples. To provide instrument flexibility and versatility, an innovative approach comprising tuning resolution by variable Resolution-Elastic Neutron Scattering (RENS) is proposed, offering further benefits by enabling systematic trading of intensity for resolution and vice versa. This study puts into evidence the advantages offered by the use of statistical chopper and of correlation technique for RENS in choosing the best compromise between resolution and beam intensity.

Introduction

Neutron probe constitutes a powerful tool in condensed matter investigations because neutrons have proper wavelengths (Angstroms) and kinetic energies (μeV to meV) to probe both the

Peer review under responsibility of Cairo University.
* Corresponding author.
E-mail address: fmigliardo@unime.it (F. Migliardo).

https://doi.org/10.1016/j.jare.2019.02.003
2090-1232/

structural and dynamical properties of material systems. X-rays interact with matter via electromagnetic interactions through atomic electron clouds (atoms have sizes comparable to the wavelength of the probing radiation). Electron beams interact with matter via electrostatic interactions, and light interacts with matter through polarizability. In contrast, neutrons interact through nuclear interactions (scattering nuclei are point particles on the scale of atomic dimensions) and have a low absorption (high penetration capability) for most elements, hence representing a unique probe for bulk. Furthermore, neutrons do not heat up or destroy samples, and the atomic neutron scattering lengths vary in a non-systematic way with atomic number. Thus, neutrons offer a series of advantages, such as the possibility of isotopic labelling and the possibility of designing sample environments with high atomic number materials.

However, neutron sources are expensive to build and maintain, are characterised by relatively low fluxes compared to synchrotrons, are not effective in investigations of rapid time-dependent processes, and require relatively large amounts of samples, which is difficult when using biological specimens.

For these reasons, instrumentation improvement and enhanced computational modelling are key components for future neutron scattering development. The latest generation neutron sources, such as the European Spallation Source (ESS), offer new opportunities to combine higher beam intensities with innovative approaches, stimulating the design of flexible neutron spectrometers to span a wide range of experimental conditions.

As a rule, Quasi Elastic Neutron Scattering (QENS) corresponds to energy transfers smaller than the incoming neutron energy, whereas Inelastic Neutron Scattering (INS) corresponds to larger energy transfers.

In Elastic Incoherent Neutron Scattering (EINS) the scattered intensity is collected at neutron energy transfer $\omega = 0$ with a given "energy resolution window" $\Delta\omega$. Compared with inelastic scattering, this contribution is higher by two or three orders of magnitude, hence providing better quality data to study small amounts of samples or small-sized samples as well as strongly absorbing samples. In this framework, the RENS technique which ultimately consists of the analysis of the EINS intensity collected at varying, as an external parameter, the instrumental energy resolution $\delta\omega$ provides an effective and innovative tool of investigation [1,2] for characterising the blurred boundary between elastic and quasi-elastic scattering. In an upgraded and revised work [3], an increasing and a decreasing sigmoidal curve described the elastically scattered intensity vs increasing instrumental energy resolution and vs increasing temperature values. Summarising, energy resolution scans at a fixed temperature and temperature scans at a fixed instrumental energy resolution of the elastic intensity furnish a complementary approach for the characterisation of system dynamical properties. The RENS approach has been experimentally tested on glycerol and sorbitol [4], trehalose/glycerol mixtures and hydrated lysozyme [5].

Following Van Hove, the time dependent pair correlation function $G(r,t)$ [6], indicates the probability to find a particle at distance r after a time t when a particle was at $t = 0$ in $r = 0$. $G(r,t)$ and the scattering function $S(Q,\omega)$ are connected in Planck's units through a time–space Fourier transform.

By introducing the instrumental resolution function $R(Q,\omega)$, the "measured" scattering law $S_R(Q,\omega)$ is the convolution of the scattering law $S(Q,\omega)$ and instrumental resolution function $R(Q,\omega)$. The time and time-space Fourier transform of the resolution function are denoted as $R(Q,t)$ and $R(r,t)$, respectively. Thus, the "measured" scattering function can be expressed as the convolution:

$$S_R(Q,\omega) = S(Q,\omega)\otimes_t R(Q,\omega) \tag{1}$$

In the general case, the resolution function in ω-space has a full width $\Delta\omega_{RES}$. Here, for the presentation of principles, the resolution function is approximated as a half period of the cosine function with full width $\Delta\omega_{RES}$ (i.e., $R(Q,\omega) = \cos(\pi\omega/\omega_{RES})$ for $|\omega| < \Delta\omega_{RES}/2$ and 0 otherwise), and the experimentally measured elastic scattering law is:

$$\begin{aligned} S_R^M(Q,\omega) &= \int_{-\frac{\Delta\omega_{RES}}{2}}^{+\frac{\Delta\omega_{RES}}{2}} S(Q,\omega-\omega')R(Q,\omega')d\omega' = \\ &= \int_{-\frac{\Delta\omega_{RES}}{2}}^{+\frac{\Delta\omega_{RES}}{2}} S(Q,\omega-\omega')\cos\left(\frac{\pi\omega'}{\Delta\omega_{RES}}\right)d\omega' \end{aligned} \tag{2}$$

For the measured elastic scattering $S_R^M(Q,\omega=0) = S_R^M(Q)$, one obtains

$$S_R^M(Q) = \int_{-\infty}^{\infty} S(Q,\omega')\cos\left(\frac{\pi\omega'}{\Delta\omega_{RES}}\right)d\omega' = I(Q,t) \;\text{ with }\; t = \frac{\pi}{\Delta\omega_{RES}} \tag{3}$$

Here, the Riemann lemma (as also used in Fresnel zone construction), which states that the integral of the product of a smooth function f and a *sine* or *cosine* function averages to zero, is used; furthermore outside the $\left(-\frac{\Delta\omega_{RES}}{2},\frac{\Delta\omega_{RES}}{2}\right)$ domain $S(Q,\omega)$ is assumed to be a smooth function in the ω variable. Furthermore, $S(Q,\omega)$ is assumed to be an even function of ω.

In RENS, the variable energy window as the scan parameter fundamentally corresponds to the physical time in the intermediate scattering function $t = \tau_{RES} = \pi/\Delta\omega_{RES}$. For the same matter, this characteristic also applies in the space-time correlation function $G(r,t)$, which describes the full structural and dynamical description of sample material. By directly revealing $I(Q,t)$, RENS is an approximate equivalent to Neutron Spin Echo (NSE) spectroscopy [7], experimentally covering the domain of shorter times than NSE but with some overlap. In practical terms, a RENS scan will contain a combination of changing the instrumental elastic resolution by changing instrumental parameters (e.g., chopper speeds) or by integrating over a number of channels in a higher resolution (i.e., smaller $\Delta\omega_{RES}$) scan. The instrumental calibration of this RENS scan is achieved by determining the same sequence of "resolution-elastic" measurements (i.e., appearing as elastic within the actually set instrumental resolution) for a truly elastic scattering standard sample, such as vanadium. As shown in an upgraded version [3], the measured elastic scattering law versus the logarithm of the instrumental energy resolution $\Delta\omega_{RES}$ follows an increasing sigmoid curve whose inflection point occurs when the instrumental resolution time matches the system relaxation time. In a numerical fitting process aimed at full depth quantitative data analysis, of course, one will use the experimentally established precise shapes of $R(Q,\omega)$ at the various resolutions involved in the RENS scan for deriving an adequate model scattering function $S(Q,\omega)$ that is consistent with the measured spectra.

Fig. 1 shows the variable energy window RENS approach achieved by integrating a measured, good energy resolution spectrum over different domains: $S_R^M(Q) = \int_{-\frac{\Delta\omega_{RES}}{2}}^{+\frac{\Delta\omega_{RES}}{2}} S_R(Q,\omega)d\omega$, which decreases towards high RENS energy resolutions, i.e., with increasing $\tau_{RES} = \pi/\Delta\omega_{RES}$. In particular, on the left column of the figure, a fixed scattering law $S(Q,\omega)$, with a Gaussian profile, and different instrumental energy resolution windows (coloured rectangles) are reported. On the right column of the figure, the integrated resolution-elastic intensity as a function of the logarithm of the instrumental resolution is shown; furthermore, the red circle with a black contour, corresponding to the fourth point, represents the curve inflection point.

For a given fixed energy resolution, the EISF contribution refers to system dynamics on a time scale longer than the instrumental time resolution. System dynamics occurring on a time scale shorter

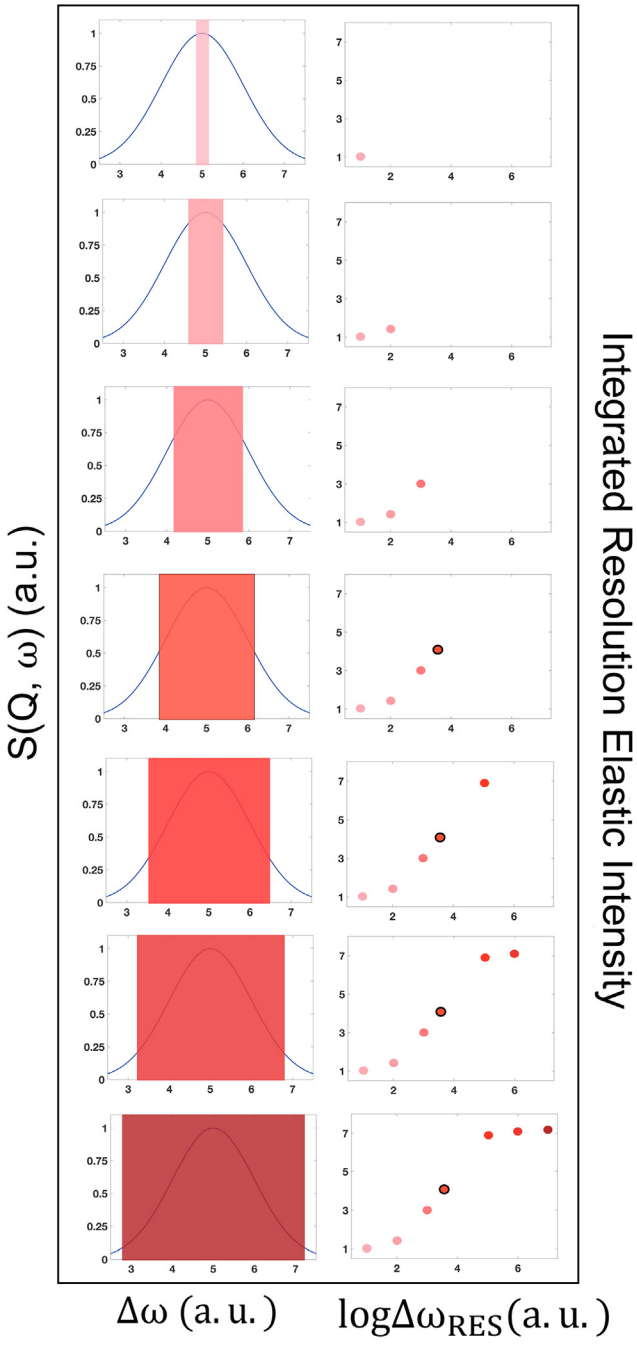

Fig. 1. Left column: fixed scattering law $S(Q,\omega)$ with variable instrumental energy resolution windows (coloured rectangles) [3]; right column: integrated resolution-elastic intensity versus logarithm of instrumental energy resolution; the red circle with a black contour (the fourth point from the left) represents the descending profile inflection point.

than the instrumental time resolution is reflected in the quasi-elastic and inelastic contributions [8–12]. In terms of the two-dimensional matrix $G(r,t)$, assuming that the resolution function $R(r,t)$ has a linewidth in time of $\tau_{RES} \propto 1/\Delta\omega_{RES}$, then matrix elements contributing to elastic scattering are those for $t > \tau_{RES}$.

Notably, a complementary way to extract quantitative information from the EINS spectra is the thermal restraint approach, which consists of maintaining fixed the instrumental energy resolution while varying the system temperature; in this case, a sigmoid behaviour whose inflection point occurs when the instrumental energy resolution matches the system relaxation time [13–15], as shown in Fig. 2.

Statistical chopper and correlation spectroscopy

Neutron correlation spectroscopy has been extensively studied in the 1960s and 1970s [16–22]. Mechanical statistical choppers were first tested and then implemented as in the case of the now decommissioned time-of-flight (TOF) spectrometer IN7 at Institute Laue Langevin (ILL) and the recently commissioned CORELLI spectrometer at Spallation Neutron Source (SNS). Correlation techniques that were initially developed in connection with steady-state neutron sources have been adapted to pulsed spallation neutron sources, allowing for the analysis of TOF spectra through their fine time modulation without corresponding monochromatisation of the beam [23,24]. More specifically, the scattering law in such a case is calculated by evaluating the cross-correlation between the measured signal and the used beam modulation sequence, which latter ideally should be of a random type [18]. Comparisons to current state of the art direct time-of-flight instruments at a steady state source, rep-rate multiplication (multiplexing) and inverted time-of-flight are reported in refs. [18,25–29].

Statistical choppers are characterised by slits and absorbing wings occupying the chopper disc perimeter [18,30–34]. The slit and wing widths are multiples of the perimeter fraction 1/n that defines the narrowest (unit) slit in the pattern (e.g., for n = 255, it is 1.4177°). The time corresponding to this angle is the chopper sequence time unit (e.g. for n = 255 at 18,000 RPM chopper rotation speed, it is 13.123 μs). In the evaluation of the correlation function, the statistical error occurring in the calculation of the correlation function is the origin of the delicate features of the method. The most relevant feature of the RENS technique is that it offers very significant gains in the data collection rate when the intensity of the elastic or quasi-elastic contribution of interest gives the major part of the integral of the whole scattering spectrum [18].

Since the beam intensity in correlation spectroscopy is independent on the resolution achieved via the random beam modulation (the time average transmission of the statistical chopper is fixed, commonly to 50%), correlation choppers offer a very flexible way of changing instrumental resolution.

To prove the feasibility and obtain a realistic estimate of the gain in efficiency achievable by cross-correlation for energy discrimination, experimental simulations have been performed by using MATLAB software.

The simplest modulation function would be a sequence of rectangular pulses with $m(t)$ equal to one or zero during equidistant time intervals (Fig. 3a). For example, the mechanical chopper uses a rotating disc with transparent slits corresponding to a pattern of type Fig. 3a. Since the slit width must be equal to the beam width for the optimum intensity, the single pulses become triangles of half width θ and multiple pulses become trapezoids (Fig. 3b). In Fig. 3, an example of a periodic pseudo-random function is shown. With mechanical disc choppers, only periodic pseudo-random pulse sequences can be produced, while truly random sequences should be aperiodic. This important boundary condition makes correlation functions ambiguous for periods of time longer than the time of revolution of the chopper disc [18].

A binary sequence (BS) is a sequence $a_0,\ldots,a_{N-1}$ of N bits, i.e., $a_j \in \{0,1\}$ for $j = 0,1,\ldots,N-1$, consisting of $m = \sum a_j$ ones and $N-m$ zeros. A BS is a Pseudo Random Binary Sequence (PRBS) if its autocorrelation function:

$$C(v) = \sum_{j=0}^{N-1} a_j a_{j+v} \tag{4}$$

has two values:

$$C(v) = \begin{cases} m, & v = 0 \\ mc, & otherwise \end{cases} \tag{5}$$

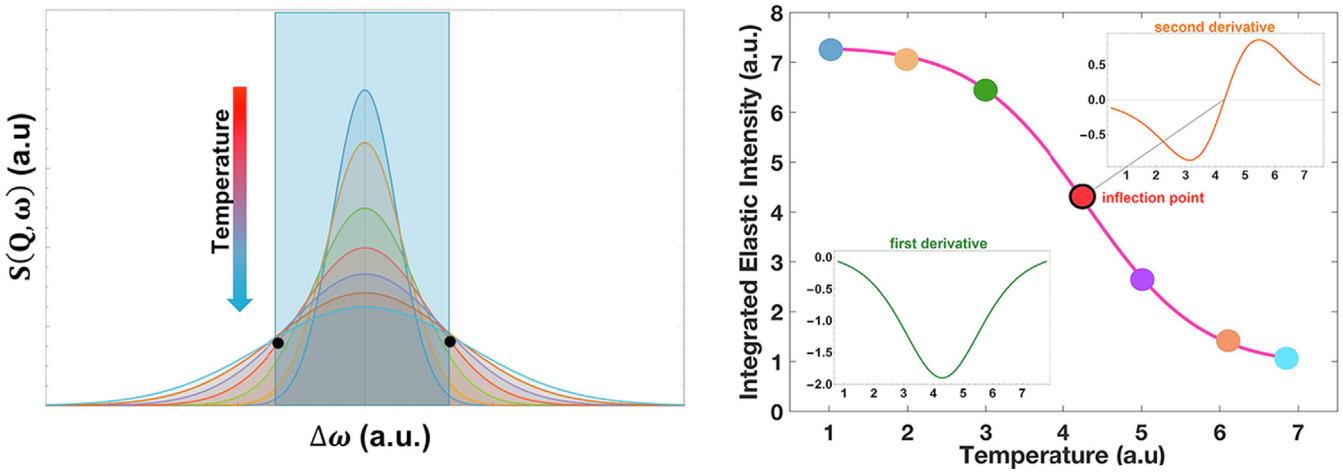

Fig. 2. Left: Thermal restraint approach consisting of maintaining fixed instrumental energy resolution (corresponding to the blue shaded area) while varying the system temperature. Right: The integrated resolution-elastic intensity shows a sigmoid behaviour whose inflection point occurs when the instrumental energy resolution matches the system relaxation time. In the inserts, the first and second derivatives are also shown, which allow us to best identify the inflection point; the second derivative passes from negative to positive signalling an ascending inflection point.

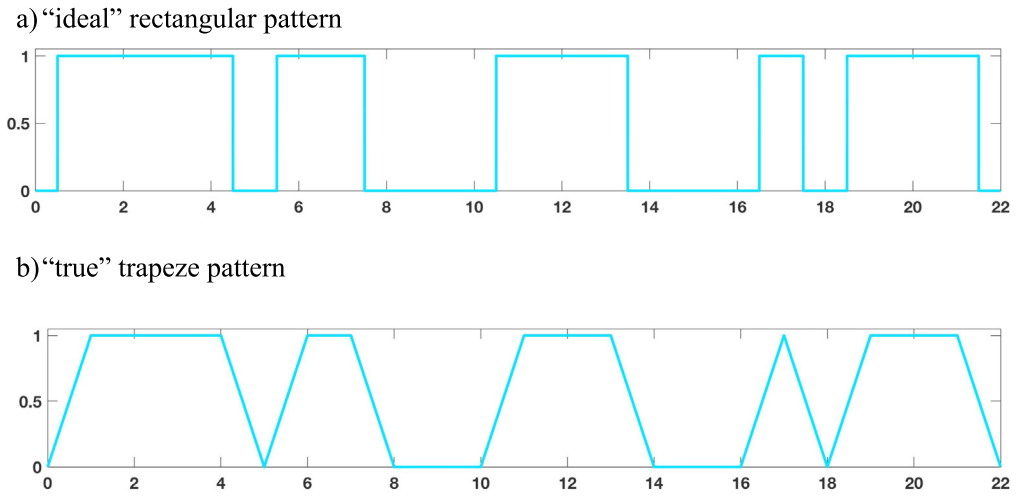

Fig. 3. Example of a periodic pseudo-random function: (a) "ideal" rectangular pattern and (b) "true" trapeze pattern.

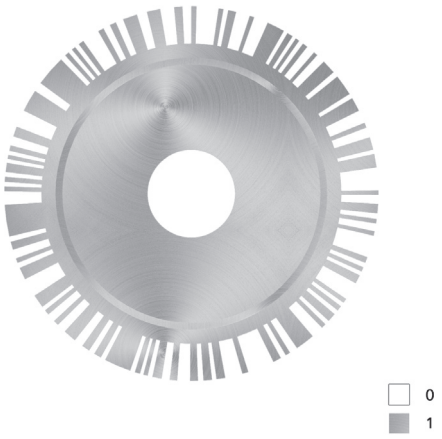

$$m(t) = [1\,0\,0\,0\,0\,0\,1\,0\,1\,1\,0\,0\,0\,1\,0\,0\,0\,1\,1$$
$$1\,1\,0\,1\,0\,1\,0\,1\,0\,0\,1\,0\,0\,1\,1\,1\,0\,1\,1\,1\,1\,1\,0\,1$$
$$1\,1\,0\,0\,0\,1\,0\,0\,1\,1\,1\,0\,1\,1\,1\,0\,0\,0\,0\,0\,1\,0\,0\,1$$
$$1\,0\,1\,0\,0\,1\,0\,0\,0\,0\,0\,1\,0\,1\,0\,1\,1\,0\,0\,0\,0\,1\,0\,1$$
$$0\,1\,1\,0\,1\,0\,0\,0\,1\,1\,1\,1\,0\,0\,1\,0\,1\,1\,0\,0\,0\,0\,0\,0$$
$$1\,0\,0\,0\,0\,1\,1\,0\,1\,1\,0\,1\,1\,0\,0\,0\,1\,0\,0\,1\,1\,0\,1\,0$$
$$1\,0\,1\,1\,1\,1\,1\,1\,0\,1\,1\,0\,1\,1\,0\,0\,1\,1\,1\,0\,0\,1\,0\,0$$
$$1\,0\,1\,1\,1\,0\,0\,0\,0\,1\,1\,1\,0\,1\,0\,0\,1\,1\,0\,1\,1\,1\,1\,1$$
$$1\,1\,0\,0\,0\,1\,0\,1\,0\,1\,1\,0\,1\,0\,1\,0\,0\,1\,1\,0\,0\,0\,0\,1$$
$$1\,1\,1\,1\,0\,0\,1\,1\,1\,1\,1\,1\,1\,0\,1\,0\,1\,0\,1\,0\,0\,0\,0\,1$$
$$0\,0\,1\,0\,0\,1\,1\,1\,0\,0\,1\,1\,1\,0\,0\,0\,1\,1\,0\,0]$$

Fig. 4. Statistical chopper (on the left) realised on the basis of the sequence reported in the table (on the right).

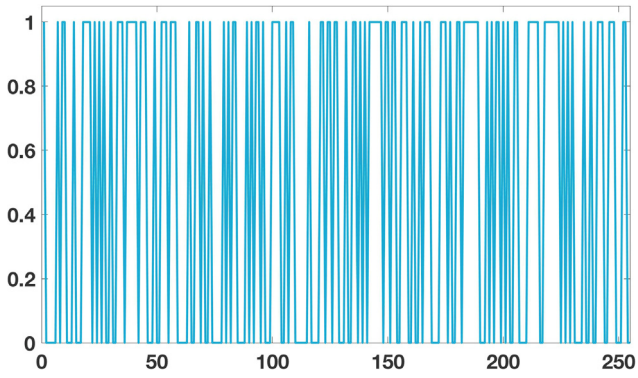

Fig. 5. "Ideal" rectangular pattern of the pseudo-random function of the statistical chopper.

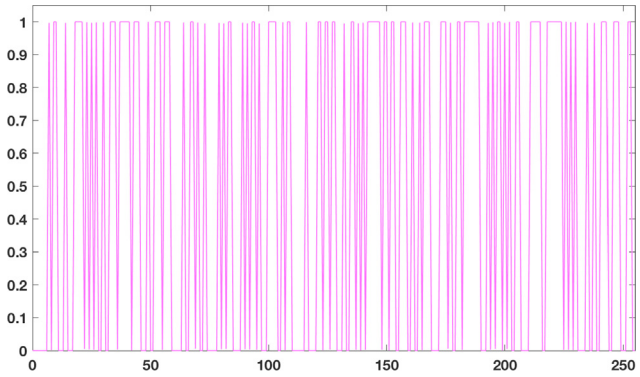

Fig. 6. "True" trapeze pattern of the pseudo-random function of the statistical chopper.

where

$$c = \frac{m-1}{N-1} \tag{6}$$

is the PRBS *duty cycle*. The PRBS is 'pseudorandom' because, although it is deterministic, it seems to be random in a sense that the value of an a_j element is independent of the values of any of the other elements, similar to real random sequences. The correlation function decreases due to the decrease of the number of sums; therefore, the sequence length can be prolonged to avoid this influence, e.g., by duplicating it.

With a statistical chopper, a pseudo-random sequence must be considered as the sequence reported in the table on the right of Fig. 4 constituted by 255 elements, equal to 2^n-1, where n = 8. This sequence gives rise to the chopper design on the left in Fig. 4 [18].

Fig. 5 shows the "ideal" rectangular linear pattern of a pseudo-random statistical chopper.

Fig. 6 shows a "true" trapeze pattern of the pseudo-random function of the statistical chopper in Fig. 4.

Fig. 7 shows a diagram of a simplified correlation technique-based instrument; the neutron beam is time-modulated by a statistical chopper following the law $m(t)$, being $0 \leqslant m(t) \leqslant 1$, while the intensity scattered by the sample is registered at a detector.

Simulation results

To examine the basic mathematical features of this approach, the process on a schematic model construction has been simulated. The above pseudo-random sequence $m(t)$, which is composed of 255 elements and a signal function $s(t)$ composed of the sum of three Lorentzian functions, is taken into account, i.e.,

$$s(t) = \frac{12.5}{0.5 + (t-80)^2} + \frac{4500}{180 + (t-120)^2} + \frac{250}{2 + (t-140)^2} \tag{7}$$

Here, t is an integer channel number for data representation. In this simplified mathematical study of the principle of correlation spectroscopy, a detailed model of a spectrometer has been not developed, where, in addition to the statistical chopper sequence $m(t)$ and the scattering function of the sample $s(t)$, the detailed geometrical layout of the spectrometer and pulse characteristics of the source together determine the detected signal $z(t)$ in a quite complex, case-by-case manner.

In the following model exploration of the principal features of correlation spectroscopy, a modulation of the signal function $s(t)$ that is correlated with the chopper transmission function $m(t)$ by simply calculating the cross-correlation function between $m(t)$ and $s(t)$ is mathematically introduced and this modulation is assumed to characterise the time dependence of the detector signal $z(t)$:

$$s(t) * m(t) = z(t) \tag{8}$$

In Fig. 8, these three functions are shown in panels (a), (b) and (c); it can be observed that the assumed detector spectrum $z(t)$ looks like random fluctuations and has no resemblance to the sig-

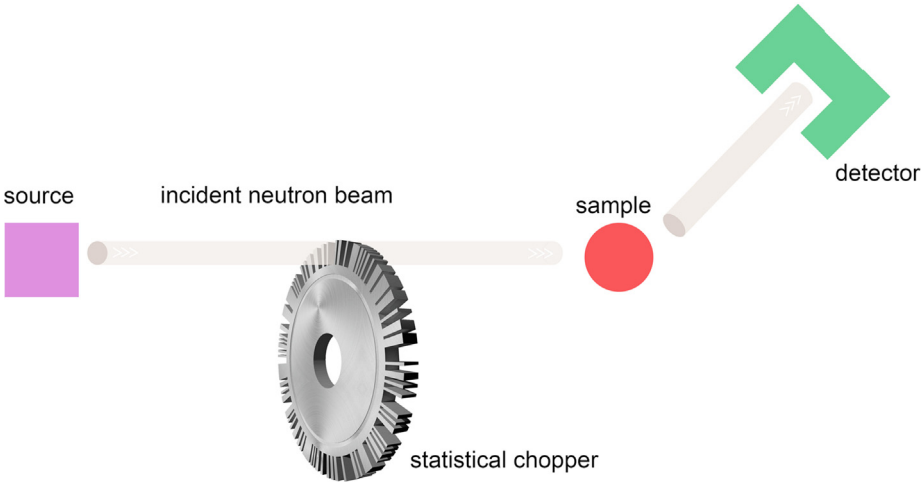

Fig. 7. Sketch of a correlation technique-based schematic instrument where a neutron beam produced by a source is intercepted by a statistical chopper before the sample, and the scattered beam is registered by the detector.

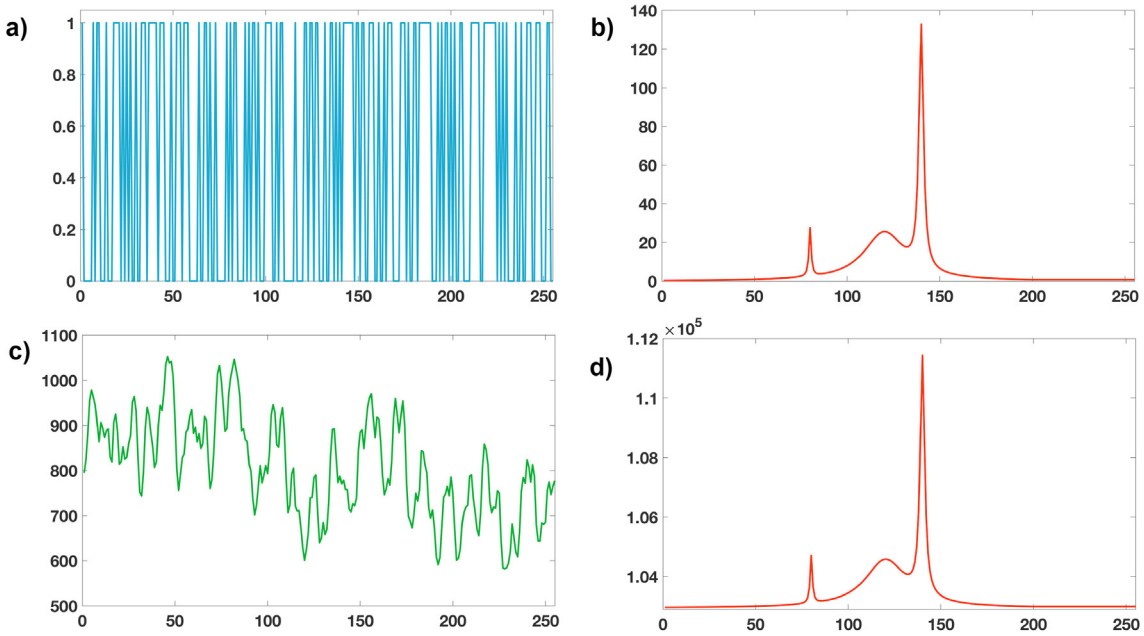

Fig. 8. (a) Function representing the pseudo-random sequence $m(t)$; (b) signal $s(t)$ constituted by the sum of three Lorentzian functions centred at $t = 80$, $t = 120$ and $t = 140$; (c) cross-correlation between $m(t)$and the signal $s(t)$ that provide the function $z(t)$; (d) the reconstructed scattering law $s(t)$obtained as the cross-correlation between $m(t)$ and $z(t)$.

nal function $s(t)$. However, the signal function can be fully recovered if the cross-correlation function between the modulation and detector signal [18] is computed:

$$z(t) * m(t) = s(t) \tag{9}$$

In order to test the validity of such an approach a set of new simulations, taking into account only one spectral contribution with an increased linewidth, have been performed. In particular, the above pseudo-random sequence $m(t)$ and three Lorentzian functions $s(t)$ centered at $t = 128$ and linewidth 0.7, 1.8 and 3.2, respectively, have been considered.

Fig. 9 reports the simulations performed with three Lorentzian functions with different widths.

In Fig. 10, a sketch of the flowchart of the simulation process leading to Fig. 8 is shown. In particular, a function $m(t)$ represents the statistical chopper and $s(t)$ the signal constituted by three Lorentzian functions. From their convolution, the signal registered

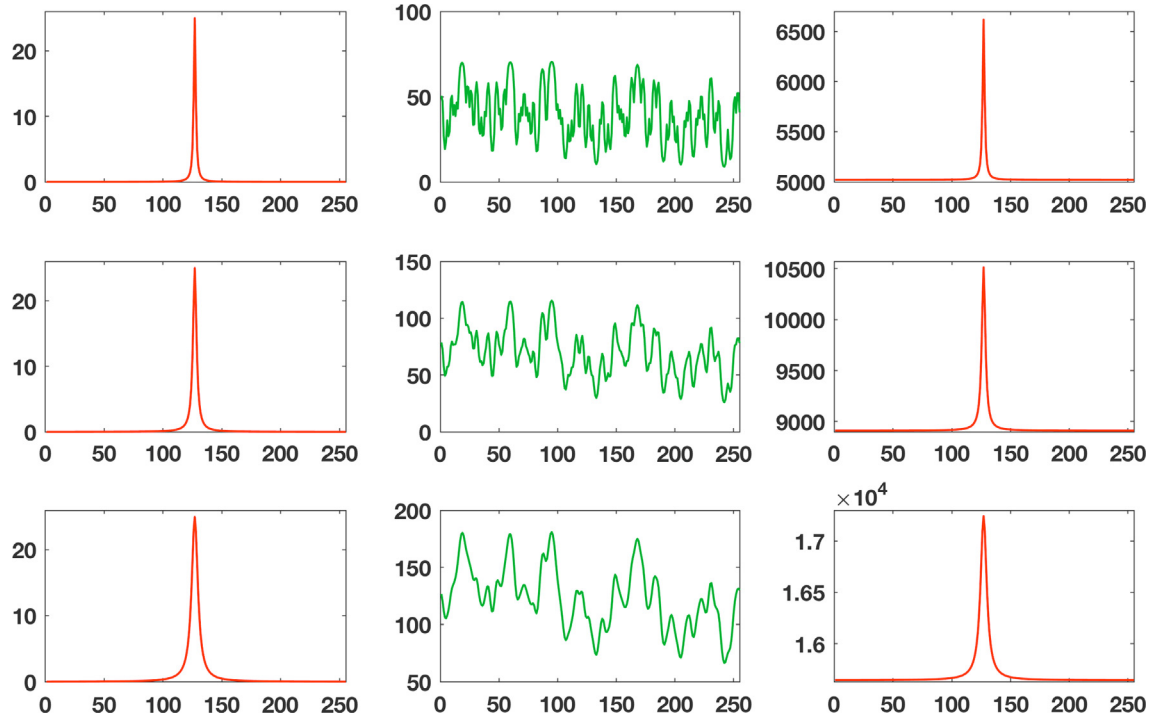

Fig. 9. Simulations performed with three Lorentzian functions with different widths: on the left the signal $s(t)$ centered at 128 with different widths, in the middle the function $z(t)$ obtained by the cross-correlation between $m(t)$ and the signal $s(t)$, and on the right the reconstructed scattering law $s(t)$provided by the cross-correlation between $m(t)$ and $z(t)$.

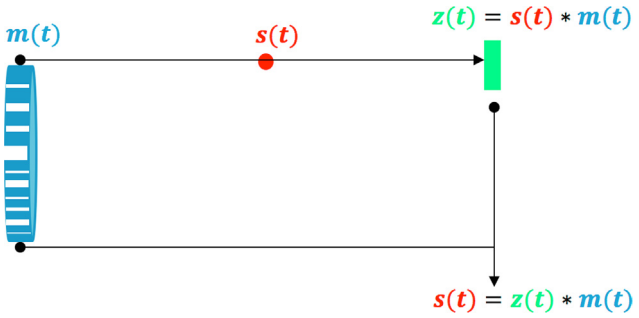

Fig. 10. Sketch of the simulation procedure. The function $m(t)$ represents the statistical chopper, and $s(t)$ is the scattering law signal. From their cross-correlation, the signal registered at the detector $z(t)$ can be obtained. Then, the cross-correlation operation between $z(t)$ and $m(t)$ reproduces the scattering law $s(t)$.

at the detector $z(t)$ can be obtained. Finally, the cross-correlation operation between $z(t)$ and $m(t)$ provides the scattering law $s(t)$.

Furthermore, as shown in a previous study [22], simulation results have been obtained for the measured conventional and statistical chopper spectra and for the calculated correlation spectra for a quasi-elastic model function with long tails in the presence of a uniform, "sample independent" background of 100 times the sample peak intensity. During the same measuring time, the signal remains unobservable next to the background created by statistical noise in conventional spectroscopy, and clearly revealed in some detail by using a statistical chopper, that provides 100 times higher incoming beam intensity on the sample for correlation based data collection. In the mentioned study, the obtained curves also could be part of a RENS experiment, with changing the quasi-elastic resolution by adding the contents of a certain number of channels. The simulation data well illustrate the decisively enhanced data collection rate obtained by the statistical chopper in the case of high intensity background compared to the sample scattering, which can e.g. be a very practical situation for samples only available in small quantities.

Conclusions

In this work, the RENS spectroscopy is described, providing evidence of the main important features. Then, it is demonstrated that the correlation neutron spectroscopy based on a statistical chopper offers significant advantages, including significant gains in beam intensity and enhanced opportunities for variable resolution studies requiring flexibility in selecting the proper balance between resolution, intensity, and sensitivity to external background.

A formulation of neutron correlation spectroscopy, which makes it possible to reconstruct neutron scattering spectra from time-modulated detected beam intensity data, is also presented. The numerical simulation results confirm the perfect reconstruction of a model scattering function for a schematic example of a beam modulation algorithm. The prominent efficiency of the correlation method in the case of the presence of very high intensity sample independent background is also shown by further simulation results.

Conflict of interest

The authors have declared no conflict of interest.

Compliance with Ethics Requirements

This article does not contain any studies with human or animal subjects.

Acknowledgements

Salvatore Magazù and Federica Migliardo gratefully acknowledge financial support from Elettra - Sincrotrone Trieste in the framework of the PIK project "Resolution-Elastic Neutron Scattering Time-of-flight Spectrometer Operating in the Repetition Rate Multiplication Mode".

References

[1] Magazù S, Migliardo F, Benedetto A. Elastic incoherent neutron scattering operating by varying instrumental energy resolution: Principle, simulations, and experiments of the Resolution Elastic Neutron Scattering (RENS). Rev Sci Instrum 2011;82. 105115-1-105115-11.
[2] Magazù S, Mamontov E. A neutron spectrometer concept implementing RENS for studies in life sciences. BBA-Gen Subj 2017;1861(1):3632–7.
[3] Magazù S, Migliardo F, Caccamo MT. Upgrading of resolution elastic neutron scattering (RENS). Adv Mater Sci Eng 2013;1. 695405-1-695405-7.
[4] Migliardo F, Angell CA, Magazù S. Contrasting dynamics of fragile and non-fragile polyalcohols through the glass, and dynamical, transitions: A comparison of neutron scattering and dielectric relaxation data for sorbitol and glycerol. BBA-Gen Subj 2017;1861(1):3540–5.
[5] Magazù S, Mezei F, Falus P, Farago B, Mamontov E, Russina M, et al. Protein dynamics as seen by (quasi) elastic neutron scattering. BBA-Gen Subj 2017;1861(1):3504–12.
[6] Hove L. Correlations in space and time and born approximation scattering in systems of interacting particles. Phys Rev 1954;95(1):249–62.
[7] Mezei F. Neutron Spin Echo: A new concept in polarized thermal neutron scattering. Zeitschrift für Physik 1972;255:146–60.
[8] Magazù S, Branca C, Migliardo F, Migliardo P, Vorobieva E, Wanderlingh U. QENS study of trehalose/water/acrylamide-acrylic acid. Phys B 2001;301(1–2):134–7.
[9] Triolo R, Arrighi V, Triolo A, Migliardo P, Magazù S, McClain JB, et al. QENS from polymeric micelles in supercritical CO_2. AIP Conf Proc 2000;513(1):234–7.
[10] Jannelli MP, Magazù S, Migliardo P, Aliotta F, Tettamanti E. Transport properties of liquid alcohols investigated by IQENS, NMR and DLS studies. J Phys Condens Matter 1996;8(43):8157–71.
[11] Magazù S. IQENS - Dynamic light scattering complementarity on hydrogenous systems. Phys B 1996;226(1–3):92–106.
[12] Magazù S, Villari V, Migliardo P, Maisano G, Telling MTF, Middendorf HD. Quasielastic neutron scattering study on disaccharide aqueous solutions. Phys B 2001;301:130–3.
[13] Migliardo F, Caccamo MT, Magazù S. Thermal analysis on bioprotectant disaccharides by elastic incoherent neutron scattering. Food Biophys 2014;9(2):99–104.
[14] Migliardo F, Caccamo MT, Magazù S. Elastic incoherent neutron scatterings wavevector and thermal analysis on glass-forming homologous disaccharides. J Non-Cryst Solids 2013;378:144–51.
[15] Magazù S, Migliardo F, Vertessy BG, Caccamo MT. Investigations of homologous disaccharidesby elastic incoherent neutron scattering and wavelet multiresolution analysis. Chem Phys 2013;424:56–61.
[16] Rosenkranz S, Osborn R. CORELLI: Efficient single crystal diffraction with elastic discrimination. Pramana-J Phys 2008;7(4):705–11.
[17] Gordon J, Kroó N, Orbán G, Pál L, Pellionisz P, Szlávik F, et al. Correlation type time of-flight spectrometer with magnetically pulsed polarized neutrons. Phys Lett A 1968;126(3):22–3.
[18] Mezei F, Caccamo MT, Migliardo F, Magazù S. Enhanced performance neutron scattering spectroscopy by use of correlation techniques. arXiv 1609.03287; 2016.
[19] Pal L, Kroo N, Pellionisz P, Szlavik F, Vizi I. Correlation-type time-of-flight spectrometer with magnetically chopped polarized neutron beam. Symposium on neutron inelastic scattering, Vol. II (IAEA Wien 1968). p. 407–16.
[20] Gompf F, Reichardt W, Gläser W, Beckurts KH. The use of a pseudostatistical chopper for time-of-flight measurements, proc. symp. on neutron inelastic scattering. Symposium on neutron inelastic scattering, Vol. II (IAEA Wien 1968). p. 417–28.
[21] Crawford RK, Haumann JR, Ostrowski GE, Price DL, Skjold K. Test of a correlation chopper as a pulsed spallation neutron source. Proceedings of ICANS-IX, Villigen 1986:365–82.
[22] Magazù S, Mezei F, Migliardo F. Correlation spectrometer for filtering of (quasi) elastic neutron scattering with variable resolution. AIP Conf Proc 1969;2018. 050006-1–050006-10.
[23] Tomiyasu K, Matsuura M, Kimura H. Modified cross-correlation for efficient white-beam inelastic neutron scattering spectroscopy. Nucl Instrum Meth 2012;677:89–93.
[24] Ye F, Liu Y, Whitfield R, Osborn R, Rosenkranz S. Implementation of cross correlation for energy discrimination on the time-of-flight spectrometer CORELLI. J Appl Cryst 2018;51:315–22.
[25] Russina M, Günther G, Grzimek V, Drescher L, Schlegel MC, Gainov R, et al. Upgrade project NEAT'2016 at Helmholtz Zentrum Berlin – What can be done on the medium power neutron source. Physica B: Cond Matter 2018;551:506–11.

[26] Russina M, Mezei F, Kozlowski T, Lewis P, Pentilla S, Fuzi J, David E, Messing G. The experimental test of the coupled moderator performance at LANSCE. Proceedings of ICANS-XVI, Jülich 2003:667–76.
[27] Russina M, Mezei F, Kali G. First implementation of novel multiplexing techniques for advanced instruments at pulsed neutron sources. J Phys Conf Ser 2012;340. 012018-1-012018-9.
[28] Sivia DS, Pynn R, Silver RN. Optimization of resolution functions for neutron scattering. Nucl Instrum Methods Phys Res Sect A 1990;287(3):538–50.
[29] Fedrigo A, Colognesi D, Bertelsen M, Hartl M, Lefmann K, Deen PP, et al. The vibrational spectrometer for the European spallation source. Rev Sci Instrum 2016;87(6). 065101-1-065101-10.
[30] Price DL, Skjold K. A detailed evaluation of the mechanical correlation chopper for neutron time of-flight spectrometry. Nucl Instrum Methods 1970;82:208–22.
[31] Von Jan R, Scher R. The statistical chopper for neutron time-of-flight spectroscopy. Nucl Instrum Methods 1970;80(1):69–76.
[32] Mook HA, Scherm R, Wilkinson MK. Search for Bose-Einstein condensation in superfluid 4He. Phys Rev A 1972;6(6):2268–71.
[33] Skoeld K. A mechanical correlation chopper for thermal neutron spectroscopy. Nucl Instr Meth 1968;63:114–6.
[34] Skjold K, Pelizzari CA, Kleb R, Ostrowski GE. Neutron scattering study of elementary excitations in liquid helium-3. Phys Rev Lett 1976;37(13):842–5.